Pathogenesis of Growth Failure and Partial Reversal with Gene Therapy in Murine and Canine Glycogen Storage Disease Type I

Elizabeth Drake Brooks[a,b], Dianne Little[c], Ramamani Arumugam[d], Baodong Sun[a], Sarah Curtis[a,b,e], Amanda DeMaster [a,b,f], Michael Maranzano[a], Mark W. Jackson[g] , Priya Kishnani[a], Michael S. Freemark[d], and Dwight D. Koeberl[a*]

[a]Division of Medical Genetics, Department of Pediatrics, Duke University Medical Center, Durham, NC, USA

[b]Division of Laboratory Animal Resources, Duke University Medical Center, Durham, NC, USA

[c]Orthopaedic Research Laboratories, Department of Orthopaedic Surgery, Duke University Medical Center, Durham, NC, USA

[d]Division of Endocrinology and Diabetes, Department of Pediatrics, Duke University Medical Center, Durham, NC, USA

[e]Current address: Rehoboth Beach Animal Hospital, Rehoboth Beach, DE USA

[f]Current address: East Lincoln Animal Hospital, Denver, NC, USA

[g]Institute of Biodiversity, Animal Health and Comparative Medicine, University of Glasgow, Scotland, UK

Running title: Growth failure in GSD-Ia animal models

* To whom correspondence should be addressed: Dr. Dwight D. Koeberl, DUMC Box 103856, Duke University Medical Center, Durham, NC 27710. Tel: (919)681-9919; FAX: (919)684-0983; Email: dwight.koeberl@duke.edu

ABSTRACT

Glycogen Storage Disease type Ia (GSD-Ia) in humans frequently causes delayed bone maturation, decrease in final adult height, and decreased growth velocity. This study evaluates the pathogenesis of growth failure and the effect of gene therapy on growth in GSD-Ia affected dogs and mice. Here we found that homozygous *G6pase* (-/-) mice with GSD-Ia have normal growth hormone (GH) levels in response to hypoglycemia, decreased insulin-like growth factor (IGF) 1 levels, and attenuated weight gain following administration of GH. Expression of hepatic GH receptor and IGF 1 mRNAs and hepatic STAT5 (phospho Y694) protein levels are reduced prior to and after GH administration, indicating GH resistance. However, restoration of G6Pase expression in the liver by treatment with adeno-associated virus 8 pseudotyped vector expressing G6Pase (AAV2/8-G6Pase) corrected body weight, but failed to normalize plasma IGF 1 in *G6pase* (-/-) mice. Untreated *G6pase* (-/-) mice also demonstrated severe delay of growth plate ossification at 12 days of age; those treated with AAV2/8-G6Pase at 14 days of age demonstrated skeletal dysplasia and limb shortening when analyzed radiographically at 6 months of age, in spite of apparent metabolic correction. Moreover, gene therapy with AAV2/9-G6Pase only partially corrected growth in GSD-Ia affected dogs as detected by weight and bone measurements and serum IGF 1 concentrations were persistently low in treated dogs. We also found that heterozygous GSD-Ia carrier dogs had decreased serum IGF 1, adult body weights and bone dimensions compared to wild-type littermates. In sum, these findings suggest that growth failure in GSD-Ia results, at least in part, from hepatic GH resistance. In addition, gene therapy improved growth in addition to promoting long-term survival in dogs and mice with GSD-Ia.

Keywords: Glycogen Storage Disease Ia; Growth Failure; Gene Therapy; Glucose-6-Phosphatase; Adeno-associated Virus; von Gierke Disease; Inherited Disorder of Metabolism; Growth Hormone; Prolactin; IGF 1; IGF 2

Abbreviations:
AAV: Adeno-associated virus
AAV-G6Pase: Adeno-associated viral vector expressing glucose-6-phosphatase
BCS: Body Condition Score
BMI: Body Mass Index
FASN: Fatty Acid Synthetase
G6Pase: Glucose 6-phosphatase
GSD-Ia: Glycogen Storage Disease Ia
GH: Growth Hormone
IGF: Insulin-like Growth Factor
PCR: Polymerase Chain Reaction
PRLR-L: Prolactin Receptor
SDS: Standard Deviation Score
STAT5: Signal Transducer and Activator of Transcription
WT: Wild-type

1. Introduction

Type Ia Glycogen Storage Disease (GSD-Ia, also known as von Gierke disease; MIM +232200) is an autosomal recessive disorder caused by a deficiency of glucose-6-phosphatase (G6Pase). This deficiency results in a number of metabolic problems such as, hypoglycemia and lactic acidosis which can lead to renal and/or hepatic disease, pancreatitis, osteopenia, hepatic adenomas or hepatocellular carcinoma and growth failure in older children and adults [1, 2].

Of humans affected with GSD-Ia, 43%-59% exhibit incongruent bone age, 10-35% short stature [3, 4], and 14% decreased growth velocity [3, 5]. There are multiple hypotheses regarding the exact cause of growth impairment, including chronic lactic acidemia, recurrent or persistent hypoglycemia, dietary restrictions, growth hormone (GH) and/or insulin-like growth factor (IGF) resistance, hypoinsulinemia, hypercortisolemia and negative calcium balance [3, 5]. Nevertheless, the pathogenesis of growth failure in GSD-Ia is poorly understood.

Several treatments have been used to improve growth of patients with GSD-Ia with variable success, but generally there are positive correlations between biochemical control of the disease, growth rate and ultimate height [2, 6]. Dietary treatment with uncooked corn starch or nasogastric tube feeding improves metabolic control and increases survival and can partially prevent growth retardation, especially if started early in life [7, 8]. Further, height standard deviation score (SDS) in children with GSD-Ia correlates with circulating IGF 2 and compliance with dietary therapy; but is not associated with a deficiency of growth hormone [3]. GH replacement therapy and diazoxide therapy improved height in some cases [9, 10]. Liver transplantation has been shown to rescue growth in the majority (8/11) of young GSD-Ia patients when recorded post-transplantation [11-13]. Inconsistent success in treatment of growth retardation and other long term complications through empirical treatment suggests that

there is an unmet clinical need for therapy that consistently improves metabolic control of GSD-Ia patients to prevent long term complications.

One such treatment under evaluation is gene therapy. Adeno-associated viral vector expressing glucose-6-phosphatase (AAV-G6Pase) to promote expression of G6Pase in the liver and kidneys has been evaluated in canine and murine GSD-Ia models [14, 15]. Animals treated with AAV-G6Pase have significantly increased survival times, normal plasma lactate and glucose, and decreased hepatic glycogen deposition and vacuolization compared to untreated GSD-Ia affected dogs or mice [14-17]. A single treatment can maintain metabolic homeostasis life-long in AAV-G6Pase-treated mice, but metabolic control wanes over time in AAV-G6Pase vector-treated dogs [16, 18]. However, GSD-Ia affected dogs receiving 2-4 treatments of AAV-G6Pase therapy with different serotypes thrive and survive to greater than 60 months of age [14, 17].

The goals of this study were to elucidate the pathogenesis of growth failure in GSD-Ia affected mice and dogs and to evaluate the effects of treatment with AAV vector-mediated therapy on growth in GSD-Ia affected mice and dogs. We used a G6Pase knockout [*G6pase* (-/-)] mouse model to clarify the role of GH signaling in the growth failure associated with GSD-Ia. We then analyzed weight gain, bone development and IGF 1 concentrations in *G6pase* (-/-) mice treated with an adeno-associated virus (AAV) vector that expresses mouse G6Pase. We evaluated bodyweight, serum IGF 1 concentrations and bone measurements in AAV-G6Pase vector-treated GSD-Ia affected dogs, GSD-Ia affected dogs only receiving dietary therapy and their unaffected wild-type and GSD-Ia heterozygous carrier littermates. Previous studies from this lab showed that this vector partially reverses G6Pase deficiency and reduces glycogen stores to near-normal levels while preventing hypoglycemia during fasting for a near normal life span of mice and dogs [14, 16]. Dog data presented were from dogs in which survival, plasma glucose and lactate, hepatic complications and vector efficacy have recently been reported by DeMaster et. al. [14].

2. Materials and Methods

2.1. Murine care and treatment

All parts of this study were performed according to the guidelines and oversight of the Duke University and North Carolina State University Institutional Animal Care and Use Committees. *G6pase* (+/-) mice were provided by Dr. Janice Chou (National Institutes of Health) and bred to produce homozygous, affected *G6pase* (-/-) offspring. Affected genotype was confirmed by polymerase chain reaction (PCR) analysis of tail DNA with primers within and flanking the neo gene insertion in the G6Pase gene as described [19]. Livers were collected from mice at 13 +/- 1 days of age and frozen on dry ice for GH-related quantification assays and Western blotting (Fig. 1, 2)**.**

Affected *G6pase* (-/-) mice were small with prominent hepatomegaly at 7 days of age, whereas unaffected carrier (+/-) and wild-type (+/+) mice appeared grossly normal. Groups of *G6pase* (-/-) and unaffected [both *G6pase* (+/+) and (+/-)] mice received daily glucose injections and were treated with GH daily for 7 days before the liver was collected for RT-PCR quantification. Unaffected mice were identified by day 3 of life by the absence of hepatomegaly, and genotype was confirmed for all mice (not shown). *G6pase* (+/+) and (+/-) mice were grouped together as normal controls. Initially, groups of 4 affected and unaffected mice were treated with 10 µg GH injected subcutaneously each morning for 7 days; later another 4 affected and unaffected mice received 25 µg daily in an equivalent manner. Ovine GH was dissolved in 10ml PBS/10% dextrose, and mice were injected subcutaneously with 100 µl/day for 7 days, starting at 7 days of age. The responses for the two dosages were equivalent, and therefore results were pooled for the two GH treatments.

The impact of hepatic G6Pase deficiency on growth was investigated further by assessing weight gain and plasma IGF 1 concentrations in *G6pase* (-/-) mice following treatment with an

adeno-associated virus (AAV) vector expressing human G6Pase ($1x10^{13}$ vector particles/kg body weight) at 2 weeks of age (Fig. 3). The vector was pseudotyped as serotype 8 to increase tropism for the liver (AAV2/8-G6Pase).

2.2. Canine care and treatment

All puppies were monitored every three to four hours for the first week of life to ensure that they were gaining weight and nursing appropriately. If they were not gaining weight, bottle or tube feeding with standard milk replacement therapy (40-100 mg/g/day) was used in conjunction with dextrose therapy to control hypoglycemia. GSD-Ia affected puppies were identified by genotyping as previously described by Kishnani et. al. [20] and administered an AAV serotype 2 vector pseudotyped as AAV9 expressing human G6Pase (AAV2/9-G6Pase) vector at 1-3 days of age ($4x10^{13}$ vector particles/kg body weight). AAV2/9-G6Pase has demonstrated good hepatorenal correction in *G6pase* (-/-) mice and was thus used in the dogs [18]. Puppies were weighed at least weekly for the first 7 weeks of life and weaned at 8 weeks of age (Fig. 4A, 4B). Adult weights were obtained after 20 months of life (Fig. 4C). For a more detailed report of puppy care, refer to DeMaster et. al. [14]. Numbers of animals lost over time were due to death of affected puppies, adoption of unaffected littermates or missed data entry (Table S1).

2.3. Murine GH-related hormone quantification assays

Total RNA was extracted from mouse tissues using RNeasy Mini Kit (Qiagen, Valencia, CA). Three μg of total RNA was reverse transcribed with 300 units of M-MLV reverse transcriptase (Life Technologies, Inc., Gaithersburg, MD) and 300 ng of random hexamer primers in a 40-μl reaction. mRNA levels were quantified with an ABI 7300 Real time PCR system, as described previously [21, 22]. For measurements of mature mRNA, all primer pairs spanned introns; amplicon lengths ranged from 90-150 bp. Thermal cycling conditions were 10 min at 95°C followed by 35-40 cycles for 15 sec at 95°C and 1 min 57°C; SYBR green incorporation into a

single peak was monitored using a dissociation curve. Expression levels were normalized against the levels of acidic riboprotein, a housekeeping gene that shows little change during cellular growth or differentiation [23]. The levels of mRNA were quantified using the comparative threshold cycle (C_T) method [24]. Table 1 shows the oligonucleotide primer pairs, all of which encode mouse genes, and C_T values obtained in mouse liver.

2.4. Serum or Plasma GH and IGF 1 concentrations

The ELISA for murine plasma GH was performed according to the manufacturer's instructions (KRC5311, Life Technologies, Grand Island, NY) or (ALPCO, Salem, NH) from mice between 10-13 days of age. The ELISA for murine plasma IGF 1 was performed according to the manufacturer's directions, except the IGF 1 standard was diluted to 10 ng/ml rather than 2 ng/ml (EA-2204, Signosis, Sunnyvale, CA). Canine serum IGF 1 concentrations were measured by a reference laboratory (Diagnostic Center for Population & Animal Health, Michigan State University, Lansing, MI) from blood taken at 8 weeks of age and between 22-23 weeks of age for two different litters (Fig. 4D). Blood was taken at 33 months of life from littermates, one GSD-Ia affected AAV2/9-G6Pase vector-treated female and two GSD-Ia carrier males remaining in the study. Animals were not fasted prior to blood collection.

*2.5. Western blottin*g

Antibodies against mouse fatty acid synthetase (FASN) (ab3844, Abcam, Cambridge, MA), c-Fos (ab7963, Abcam), signal transducer and activator of transcription (STAT5) (phospho Y694) (ab32364, Abcam), and β-actin (ab20272, Abcam) were used for Western blotting analysis (Fig. 2A, B). Western blot was performed in the same manner described in Sun et. al. 2005 [25].

2.6. Canine body weight analysis

Body weights were extracted from the medical records retrospectively over the course of several years for GSD-Ia affected dogs treated with AAV2/9-G6Pase (n=8) 1-3 days after birth, GSD-Ia affected dogs treated only with dietary supplementation from birth (n=7) and unaffected littermates (n=22) for the first 7 weeks of life (Fig. 4A, B, Table S1). Adult (20 months – 9 years of age) body weights were obtained from medical records of GSD-Ia AAV2/9-G6Pase vector-treated dogs currently in the study (n=4, 3 male, 1 female), dogs in the GSD-Ia carrier breeding colony (n=10, 4 male, 6 female) or as reported by owners from those unaffected dogs that were adopted out of the study, containing both carrier (n=5, 1 male, 4 female) and wild-type dogs (n=4, 4 males) (Fig. 4C). Body condition score (BCS) was determined based on a 9-point scale by Duke University animal care staff or the owners based on the “Body Condition System” chart by Nestlé Purina (St. Louis, Missouri) [26].

2.7. Mouse limb staining

12-day-old mouse tissues were collected from whole *G6pase* (-/-) and wild-type mice that were frozen and stored in -80°C, mice were then thawed, imaged by high resolution radiography (methods below) and then skin was removed from limbs and tail. Limbs were then stained whole using Alcian blue for cartilage and Alizarin red for bone according to methods found in Yamazaki et. al. 2011 [27] (Fig. 5).

2.8. Murine radiographic measurements and analysis

Radiographs of mice were taken of euthanized *G6pase* (-/-) and wild-type mice at 12 days or at 6 months of life using a model MX20 Faxitron machine (Faxitron X-ray Corporation, Wheeling, IL) and processed with Dalsa specimen radiography system version 1.0 (Dalsa life sciences, Tucson, AZ). Mice were imaged in right and left lateral, ventrodorsal and dorsoventral positions to obtain high resolution images of the axial and appendicular skeleton (Fig. 6). All radiographs

were measured independently by two trained graders measuring bone lengths using Image J (Wayne Rasband, National Institutes of Health, USA) (Fig. S1).

2.9. Canine radiographic measurements and analysis

Radiographs were taken of dogs with an InnoVet select E7242x x-ray machine (Summit Industry, Chicago, IL) and processed using an IDEXX-CR 1417 digital imaging system (IDEXX Laboratories, Inc., Westbrooke, ME). Bone dimensions were measured from radiographs taken using right and left lateral, ventrodorsal and dorsoventral positioning of animals.

Radiographs of 3-month-old male dogs under brief physical restraint were taken of the front legs due to intermittent forelimb lameness noted in a male GSD-Ia affected dog treated with AAV2/9-G6Pase on the first day of life, radiographs of a male wild-type littermate were obtained at the same time for comparison. These radiographs were measured retrospectively; several measurements were not obtainable due to variation in procedure and poor positioning. Radiographs of a 3-month-old female GSD-Ia carrier in a different litter were obtained under sedation for comparison (Fig. 7A, Tables S2, S3).

Photographs were taken of a 34-month-old GSD-Ia affected female dog who had been treated with AAV2/9-G6Pase at 1 day of age and retreated with AAV2/8-G6Pase at 15 months of age and her male GSD-Ia heterozygous littermate, who had also received AAV2/9-G6Pase at 1 day of age (Fig. 7B, Table S4).

Radiographs were performed under sedation on the same GSD-Ia affected female dog above at 37 months of age and a different male GSD-Ia heterozygous littermate, who had also received AAV2/9-G6Pase at 1 day of age (Fig. 7C-E, Tables S2, S4). All radiographs were measured independently by two trained graders measuring calibrated bone lengths and widths using ClearCanvas Workstation 2.0 (Toronto, ON, Canada). Graders varied from a 0.02 mm to 5.91

mm difference in individual bone measurements, with a mean 0.83 ± 1.01 mm difference. Measurements were averaged between graders and included in supplemental tables 3 and 4.

2.10. Statistical Analysis

A two-tailed homoscedastic Student's *t*-test was used to determine significant differences in measurements between *G6pase* (-/-) mice and wild-type mice. A one-tailed heteroscedastic Student's *t*-test was used to compare between weights at each time point for the GSD-Ia canine growth curve (Fig. 4A, 4B). Kruskal-Wallis Test was used to determine significance of mouse radiographic bone lengths (Fig. S1). One way between subjects ANOVA with Tukey analysis was used to compare IGF 1 values and adult body weights between wild-type, GSD-Ia carriers and GSD-Ia affected dogs treated with AAV2/9-G6Pase (Fig. 4C, 4D). P values less than 0.05 were considered significant.

3. Results

3.1. Murine GSD-Ia hepatic GH signaling and IGF production

As shown in Figure 1A, randomly sampled plasma GH concentrations in *G6pase* (-/-) mice not treated with glucose injections (UT) were comparable to those in wild-type controls. However, GH concentrations were decreased in glucose-treated *G6pase* (-/-) mice (Fig. 1A; GT) indicating either suppression from glucose therapy or a general GH deficiency. Plasma GH concentrations in young, glucose-treated, unaffected mice varied from <1 to 41 ng/ml (11 ± 16 ng/ml; n=6; not shown), indicating that this type of glucose treatment may suppress GH as expected in some mice, but not all. These findings suggest that regulation of pituitary GH secretion is largely preserved in GSD-Ia. On the other hand, plasma IGF 1 levels were reduced in neonatal *G6pase* (-/-) mice (Fig. 1B), suggesting that GH induction of IGF 1 expression may be attenuated. Support for this hypothesis was provided by studies of basal levels of GHR-L receptor, PRLR-L

receptor, and IGF 1 mRNAs, which reduced by 55-70% ($p<0.01$) in untreated neonatal *G6pase* (-/-) mice. In contrast, hepatic expression of IGF 2 mRNA was normal (Fig. 1C).

Moreover, hepatic levels of phosphorylated STAT5 (phospho Y694) and c-Fos were reduced in both glucose-treated and untreated *G6pase* (-/-) mice compared with *G6pase* (+/+) mice, consistent with decreased hepatic GH signaling [28] (Fig. 2A, B). Accordingly, the administration of GH and glucose caused little or no increase in hepatic IGF 1 mRNA in GT *G6pase* (-/-) mice compared with *G6pase* (+/+) mice (Fig. 2D), and GH-stimulated weight gain was blunted in comparison to that observed in wild-type mice: GH treatment for 7 days increased body weight by 38% ($p<0.02$) in unaffected [*G6pase* (+/+) and (+/-)] controls but had no significant effect in *G6pase* (-/-) mice (Fig. 2C).

3.2. AAV2/8-G6Pase administration to G6pase *(-/-) mice rescues adult growth, but not plasma IGF 1*

The GSD-Ia liver features massive accumulation of lipids as well as glycogen [29]. Accordingly, hepatic FASN was increased in *G6pase* (-/-) mice (Fig. 2A-B) [30]. AAV2/8-G6Pase administration increased hepatic G6Pase activity, reduced glycogen accumulation to the levels observed in wild-type mice, and prevented fasting hypoglycemia [16], however, the weight gain of vector-treated *G6pase* (-/-) mice was significantly decreased at 1 month in comparison with wild-type controls (Fig. 3A). Body weight normalized by 2-3 months and plasma IGF 1 in the *G6pase* (-/-) mice was not significantly reduced at 2 months of age, indicating an initial improvement from AAV2/8-G6Pase therapy (Fig. 3B). However, *G6pase* (-/-) plasma IGF 1 was significantly decreased at 4 and 6 months of age while body weight trended lower in comparison with wild-type mice at 6 months of age without reaching statistical significance (Fig. 3A).

3.3. AAV2/9-G6Pase administration to GSD-Ia affected dogs partially rescues growth compared to dietary therapy alone

GSD-Ia affected dogs receiving only dietary treatment were 70% (214 ± 34 g, n=6) of the weight of AAV2/9-G6Pase vector-treated dogs (307 ± 100 g, n=8, p=0.02) at 1 week of age and only 54% (565 ± 15 g, n=2) of weight of AAV2/9-G6Pase vector-treated dogs (1038 ± 226 g, n=7, p<0.001) at 7 weeks of age (Fig. 4A). Neonatal AAV2/9-G6Pase therapy increased growth rate of GSD-Ia dogs compared to dietary therapy alone, but growth curves of these animals did not parallel those of unaffected littermates at any time in the 7 week study period (Fig. 4B). For example, AAV2/9-G6Pase treated dogs were 61% of unaffected littermates' weight (502 ± 118 g, n=22, p=0.0002) at 1 week of age and 48% the weight of unaffected littermates (2153 ± 472 g, n=22, $p=2.18X10^{-8}$) at 7 weeks of age. Bodyweights of wild-type and GSD-Ia heterozygous carriers were not significantly different (p>0.11) during the 7 weeks, and were therefore grouped together as an unaffected littermate group (Fig. 4B). There was, however, some minor divergence of growth curves beginning at 5 weeks of age between wild-type and GSD-Ia carriers (not shown).

3.4 Adult AAV2/9-G6Pase vector-treated GSD-Ia affected dogs and GSD-Ia carriers are smaller than adult wild-type littermates.

At 34 months of age, a GSD-Ia affected AAV2/9-G6Pase vector-treated female dog was grossly smaller in size and stature (Fig. 7B) and weighed 46% (3.8 kg) of the weight of her heterozygous GSD-Ia carrier male littermate (8.2 kg). Among adult dogs (20 months – 9 years of age), AAV2/9-G6Pase treated dogs (n=4) averaged 3.9 ± 0.8 kg body weight, while their wild-type littermates (n=4) averaged 13.8 ± 2.2 kg body weight , whereas, GSD-Ia carriers averaged 8.1 ± 2.8 kg body weight (n=15) (Fig. 4C). BCS was not statistically significant among all dogs based on a 9-point scale, ranging from 3.5 to 6 (not shown).

3.5. AAV2/9-G6Pase treatment does not rescue serum IGF 1 concentrations in GSD-Ia affected dogs and GSD-Ia carrier dogs have reduced serum IGF 1 compared to wild-type littermates.

Serum IGF 1 was 1.7 ± 0.6 nmol/L in AAV2/9-G6Pase treated GSD-Ia dogs (n=3, 2 male, 1 female), 15.3 ± 5.2 nmol/L in GSD-Ia carrier dogs (n=4, 2 male, 2 female) in comparison with 43.5 ± 7.8 nmol/L in their male wild-type littermates (n=2 $p<0.001$) at 8 weeks of age (Fig. 4D). At 22-23 weeks of age, serum IGF 1 was 2.7 ± 2.1 nmol/L in the same GSD-Ia dogs (n=3); 14.8 ± 7.0 nmol/L in the same GSD-Ia carrier dogs (n=4 $p=0.018$) and 27 nmol/L in a wild-type littermate. At 33 months of age, serum IGF 1 levels were 1.0 nmol/L in a female AAV2/9-G6Pase treated GSD-Ia dog (n=1) and 10.5 ± 2.1 nmol/L in her carrier male littermates (n=2) (Table S2).

Normal canine IGF 1 reference range from the reference laboratory was 4-95 nmol/L (31-725 ng/ml), but spans a wide variety of ages and breeds. Based on data from Greer et al, normal IGF 1 concentrations for dogs of the size and age of the dogs in the current study should be between 20-320 ng/ml (3-42 nmol/L) [31]; whereas, data from Jaillardon et al indicates IGF 1 for adult dogs <15 kg (n=177) ranges from 21-433 ng/ml (3-57 nmol/L) with a mean of 117 ng/ml (15 nmol/L), and no significant difference in IGF 1 with age [32].

3.6. Delayed ossification of G6pase *(-/-) mice and dysplasia and decreased bone dimensions in AAV2/8-G6Pase vector-treated* G6pase *(-/-) mice*

Alcian Blue and Alizarin Red staining of whole limbs in 12-day-old *G6pase* (-/-) mice compared to wild-type mice demonstrated delay in ossification of the femoral head, delay in development of secondary centers of ossification in the physes of the distal femur and proximal tibia, and dysplasia of the elbow, with delayed physeal closure and abnormal angulation of the distal humerus resulting in incongruence of the distal humerus relative to the proximal radius and ulna. Abnormal metaphyseal morphology of the proximal radius was also noted (Fig. 5).

Hip radiographs of four groups of mice (Fig. 6A) confirmed delay in ossification of the femoral head in 12-day-old *G6pase* (-/-) mice, and dysplasia of the hip and exaggerated development of

the third trochanter in 6-month old *G6pase* (-/-) AAV2/8-G6Pase vector-treated mice. Knee radiographs (Fig. 6B) demonstrated thickening and irregularity of the metaphyseal growth plate of the proximal tibia and distal femur, with delay in development of secondary centers of ossification in 12-day-old *G6pase* (-/-) mice compared to unaffected controls. In 6-month-old mice, there was irregularity and flattening of the femoral condyles, and bowing of the fibulae of *G6pase* (-/-) AAV2/8-G6Pase vector-treated mice compared to unaffected. In caudal vertebrae 4-6 (Fig. 6C), besides shortening of the vertebrae in both affected groups, there was premature mineralization of the caudal intervertebral discs in the tail in 6-month-old *G6pase* (-/-) AAV2/8-G6Pase vector-treated mice. This abnormality was observed only in the proximal 1/3 of the tail. In the shoulder (Fig. 6D), elbow (Fig. 6E) and carpus/wrist (Fig. 6F), there was severe dysplasia in *G6pase* (-/-) 12-day-old mice, with widening and irregularity of the metaphyseal growth plates and impaired development of secondary centers of ossification, with premature severe arthritis evident in 6-month-old *G6pase* (-/-) AAV2/8-G6Pase vector-treated mice compared to unaffected mice of similar age. Enthesiopathies were also evident, particularly at the deltoid tuberosity of the proximal humerus, where widening and lengthening was noted in 6-month-old *G6pase* (-/-) AAV2/8-G6Pase vector-treated mice compared to unaffected mice of similar age. In hips (Fig. 6A), knees (Fig. 6B) and elbows (Fig. 6E) of 6-month-old *G6pase* (-/-) AAV2/8-G6Pase vector-treated mice, the trabecular bone pattern of the proximal femur, patella, distal femur, proximal tibia, distal humerus and olecranon was enhanced, and there was increased cortico-medullary contrast in the proximal femur and patella, suggestive of some degree of osteoporosis.

Long bones of the extremities were uniformly shorter in *G6pase* (-/-) mice compared with wild-type at both 12 days and 6 months of life (Fig. S1A). The long bones in weight bearing digits (the third metatarsals and phalanges) showed a significant difference between *G6pase* (-/-) mice and unaffected mice at both 12 days and 6 months of age, whereas the bones in non-

weight bearing digits were not significantly different between GSD-Ia in 6-month-old mice, despite the difference between both groups at 12 days of age (Fig. S1B). The heads and third cervical vertebrae of mature *G6pase* (-/-) mice are smaller than unaffected mice, but other vertebrae, ilium and ischium are not significantly different in 6-month-old vector treated mice (Fig. S1C).

3.8. Bone dimensions were decreased in AAV2/9-G6Pase treated GSD-Ia affected dog and GSD-Ia carrier compared to wild-type.

At 3 months of age, forelimb long bone dimensions of an AAV2/9-G6Pase treated GSD-Ia affected male dog were smaller than those of a male wild-type littermate, while long bone dimensions of a female GSD-Ia carrier were also smaller than that of the male wild-type. Long bone dimensions of the AAV2/9-G6Pase treated GSD-Ia affected male dog at this age were also smaller than the female GSD-Ia carrier of the same age (Fig. 7A, Table S3). The wild-type dog weighed 3.9 kg, the GSD-Ia carrier weighed 3.2 kg, and the GSD-Ia AAV2/9-G6Pase dog weighed 1.8 kg at time radiographs were taken.

At 37 months of age, long bone dimensions, pelvic dimensions and vertebral dimensions of an AAV2/9-G6Pase treated GSD-Ia affected female dog were smaller than those of a GSD-Ia carrier male littermate (Fig. 7C-E, Table S4). Dogs weighed 3.8 kg and 8.6 kg, respectively, at time of radiographs. Radiographs of wild-type animals at this age were not available for comparisons because they had left the study.

4. Discussion

4.1. Proposed pathogenesis of growth failure in GSD-Ia

The pathogenesis of growth failure in glycogen storage disease is complex; contributing factors may include restricted diet, acidosis, hypercortisolemia (from recurrent hypoglycemia [5]), and

hepatic and renal insufficiency. Here we explored the role of hepatic GH signaling and IGF production in GSD-Ia using a G6Pase deficient mouse model. We showed that hepatic IGF 1 mRNA levels and plasma IGF 1 concentrations are low despite normal randomly sampled GH concentrations, and body weight gain fails to increase in response to exogenous GH. These observations suggest that GSD-Ia is associated with hepatic GH resistance. The low levels of phosphoSTAT5 and c-Fos in liver and the failure of hepatic IGF 1 mRNA to rise in response to GH treatment provides strong support for this hypothesis.

The GH resistance of mice with G6Pase deficiency results, at least in part, from a reduction in liver GH receptor expression. In theory, the decrease in GH receptor expression might be caused by hepatic inflammation induced by excess glycogen and/or lipid accumulation or might reflect a defect in GH receptor transcription related to dysfunctional intracellular glucose metabolism. *G6pase* (-/-) mice also had reductions in hepatic PRL receptors which activate STAT5 in rat liver, albeit with considerably lower potency than GH [33]. Thus the reduction in PRL receptor expression may contribute slightly to the fall in phospho STAT5 in livers of G6Pase deficient mice. However, PRL, in contrast to GH, does not induce hepatic IGF 1 production [34, 35].

4.2. Role of IGF 1 on bone development.

We noted delayed ossification in *G6pase* (-/-) mice at 12 days of age likely due to the decrease in IGF 1. IGF 1 increases cell proliferation and protein synthesis and can stimulate long bone growth [36], probably through its effects on chondrocyte proliferation and hypertrophy [37-39]. However, IGF 1 action at the level of the chondrocyte is regulated by a complex series of paracrine and autocrine feedback loops [38], such that the impact of low serum IGF 1 on chondrocyte proliferation in the current study is unknown. Depletion of IGF 1 and a key serum stabilizer of serum IGF 1 leads to growth retardation in several mouse studies, but hepatic-

specific depletion of IGF 1 alone does not impair growth [40]. However, the marked increase in growth velocity in patients after liver transplantation suggests that there may be at least some endocrine effect of normalized serum IGF 1 on recovery of growth [11-13]. As far as we know, there are no reports of IGF 1 concentrations before and after liver transplantation in GSD-Ia patients.

In contrast to IGF 1, hepatic IGF 2 mRNA levels in the *G6pase* (-/-) mice were normal; this is not surprising, given the variable reductions in serum IGF 2 in patients with GH deficiency and the limited (or lack of) effect of GH treatment on circulating IGF 2 levels in children and adults [41-43].

4.3. AAV-G6Pase therapy fails to fully correct growth failure in GSD-Ia canine and murine models.

Partial reconstitution of hepatic G6Pase through AAV vector transduction promoted weight gain in *G6pase* (-/-) mice after a delay of 2-6 weeks; interestingly, plasma IGF 1 concentrations declined after 2 months of age, suggesting that GH resistance persists despite catch-up weight gain. It is of note that the initial delay in weight gain in GSD-Ia mice occurs during the period prior to and during expected sexual maturation; this may explain in part the delayed puberty and late catch-up growth observed in many children and teenagers with glycogen storage disease. We also found that administration of AAV2/9-G6Pase to GSD-Ia dogs within 3 days of birth partially rescues growth compared to dietary therapy, as assessed by bodyweight, but fails to rescue serum IGF 1 or bone dimensions. Our findings are consistent with clinical studies showing that height z score correlates positively with plasma IGF 1 concentrations and inversely with GH levels in children with various forms of glycogen storage disease [5, 44].

4.4. Timing of AAV2/9-G6Pase administration relative to development.

The reasons for failure of AAV2/9-G6Pase treatment administered in the neonatal period (day 1-3 post-partum) to fully correct growth failure in dogs and mice are unknown and are likely multifactorial and complex. That normal weight gain can be achieved following administration of AAV-G6Pase therapy during infancy in mice, but not in dogs suggests differences in comparative development between dog and mouse may play a role. In the mouse, dog and human, the appearance of the proximal epiphysis of the humerus occurs at postpartum day 5-10, week 1-2, and as early as gestational week 36-40, respectively [45], suggesting different absolute rates of skeletal development across species. This has been shown to occur in the nervous system across species [46], but similar cross-species modeling has not yet been applied to specific markers of hepatic or musculoskeletal development, which is likely to be more difficult given axial-appendicular and craniad-caudad developmental gradients. For example, we found that fewer structures in the caudal component of the axial skeleton demonstrated persistent shortening than in the craniad axial skeleton in AAV 2/8-G6Pase vector-treated mice (Fig. S1D) suggesting that timing of administration of treatment in GSD-Ia affected mice was appropriate to rescue growth in the caudad component of the axial skeleton, but was delayed relative to growth correction in the craniad axial skeleton.

4.5. Heterozygous GSD-Ia carriers demonstrate growth deficiency

Although canine carriers for GSD-Ia do not appear to exhibit overt clinical signs, they do demonstrate metabolic abnormalities and growth deficiencies. Weinstein et al. have demonstrated that there is about a 50% decrease in hepatic G6Pase activity, increased hepatocellular glycogen and an increase in blood lactate after 12 hours of fasting in GSD-Ia carrier animals compared with wild-type dogs [17]. We also demonstrated deceases in IGF 1 concentrations in carrier dogs in comparison to wild-type dogs (Fig. 4D) as well as decreases in adult body weight (Fig. 4C). However, to our knowledge, metabolic and growth abnormalities have not been demonstrated in carrier parents of affected GSD-Ia human patients.

4.6. Summary

Our findings indicate that growth failure and IGF 1 deficiency of GSD-Ia appears to result, at least in part, from hepatic resistance to GH action. As noted here, gene therapy of GSD-Ia affected dogs and mice can prolong survival, prevent fasting hypoglycemia, and reduce hepatic steatosis but fails to normalize bone growth and IGF 1 production [14, 16, 17, 47, 48]. It is possible that more effective gene therapy at an early time point would fully normalize hepatic G6Pase expression, reverse hepatic-based GH resistance, and normalize growth [16, 17, 48]. Until more effective gene vectors are developed, the therapy of growth failure in GSD-Ia remains focused on dietary measures. Given the state of GH resistance, GH treatment alone is not likely to be effective; the potential benefits of IGF 1 therapy remain to be explored. Our data will guide future studies in dog and mouse models to assess the endocrine, paracrine and autocrine effects of IGF 1 and growth hormone in GSD-Ia to develop the best method and timing of intervention to prevent growth failure in AAV-G6Pase treated GSD-Ia affected individuals.

ACKNOWLEDGEMENTS

This work was funded in part by the Children's Fund for GSD Research, the Association for Glycogen Storage Disease, Alice and YT Chen Center for Pediatric Genetics and Genomics, For the Love of Christopher, and the Duke Children's Miracle Network. Dr. Little received support from NIAMS (K08AR059784). Drs. Freemark and Arumugam received support from the NICHD (HD24192), American Diabetes Association, and Duke Children's Miracle Network. We deeply appreciate the dedication shown by Duke Vivarium, when caring for the *G6pase* (-/-) mice and GSD-Ia dog colony. Much appreciation is also due to Dr. Shannon Smith, Ms. Songtao Li, Mr. Andrew Bird, Mr. Dustin J. Landau, Ms. Hiruni Amarasekara, and Ms. Maggie Chu for technical assistance and the extremely dedicated dog feeding crew. A special thanks is extended to all those that adopted unaffected dogs out of the study and provided additional data, including Dr. Kyha Williams, Laura Jordan, Jeff Lee, Arnette Williams, the Bird Family, Kieran Hendricksen, Dr. Baodong Sun, Deborah King, Janet Steele, Krista Beck, Christian Marsini and Randy Amoako. The authors acknowledge the helpful comments of Drs. Farshid Guilak and Y.-T. Chen on this work, as well as Dr. Kent Refsal for his information regarding IGF 1 testing in dogs.

The authors have no conflicts of interest to report with regard to this work.

REFERENCES

[1] D.D. Koeberl, P.S. Kishnani, D. Bali, Y.T. Chen, Emerging therapies for glycogen storage disease type I Trends in endocrinology and metabolism: TEM 20 (2009) 252-258.

[2] D.A. Weinstein, J.I. Wolfsdorf, Effect of continuous glucose therapy with uncooked cornstarch on the long-term clinical course of type 1a glycogen storage disease European journal of pediatrics 161 Suppl 1 (2002) S35-39.

[3] D. Melis, R. Pivonello, G. Parenti, R. Della Casa, M. Salerno, F. Balivo, P. Piccolo, C. Di Somma, A. Colao, G. Andria, The Growth Hormone-Insulin-like Growth Factor Axis in Glycogen Storage Disease Type 1: Evidence of Different Growth Patterns and Insulin-like Growth Factor Levels in Patients with Glycogen Storage Disease Type 1a and 1b J Pediatr-Us 156 (2010) 663-U198.

[4] J.P. Rake, G. Visser, P. Labrune, J.V. Leonard, K. Ullrich, G.P. Smit, Glycogen storage disease type I: diagnosis, management, clinical course and outcome. Results of the European Study on Glycogen Storage Disease Type I (ESGSD I) European journal of pediatrics 161 Suppl 1 (2002) S20-34.

[5] H.R. Mundy, P.C. Hindmarsh, D.R. Matthews, J.V. Leonard, P.J. Lee, The regulation of growth in glycogen storage disease type 1 Clin Endocrinol 58 (2003) 332-339.

[6] B. Schwahn, F. Rauch, U. Wendel, E. Schonau, Low bone mass in glycogen storage disease type 1 is associated with reduced muscle force and poor metabolic control The Journal of pediatrics 141 (2002) 350-356.

[7] S. Dagdelen, A. Atmaca, A. Alikasifoglu, T. Erbas, Pituitary hypoplasia and growth hormone deficiency in a woman with glycogen storage disease type Ia: a case report Journal of medical case reports 2 (2008) 210.

[8] J.I. Wolfsdorf, C.R. Rudlin, J.F. Crigler, Jr., Physical growth and development of children with type 1 glycogen-storage disease: comparison of the effects of long-term use of dextrose and uncooked cornstarch The American journal of clinical nutrition 52 (1990) 1051-1057.

[9] R.A. Noto, V. Vijayaraghavan, A. Timoshin, D. Sansobrino, Improved growth with growth hormone therapy in a child with glycogen storage disease Ib Acta Paediatr 92 (2003) 977-979.

[10] J.M. Nuoffer, P.E. Mullis, U.N. Wiesmann, Treatment with low-dose diazoxide in two growth-retarded prepubertal girls with glycogen storage disease type Ia resulted in catch-up growth Journal of inherited metabolic disease 20 (1997) 790-798.

[11] L. Faivre, D. Houssin, J. Valayer, J. Brouard, M. Hadchouel, O. Bernard, Long-term outcome of liver transplantation in patients with glycogen storage disease type Ia Journal of inherited metabolic disease 22 (1999) 723-732.

[12] D. Matern, T.E. Starzl, W. Arnaout, J. Barnard, J.S. Bynon, A. Dhawan, J. Emond, E.B. Haagsma, G. Hug, A. Lachaux, G.P. Smit, Y.T. Chen, Liver transplantation for glycogen storage disease types I, III, and IV European journal of pediatrics 158 Suppl 2 (1999) S43-48.

[13] S.G. Iyer, C.L. Chen, C.C. Wang, S.H. Wang, A.M. Concejero, Y.W. Liu, C.H. Yang, C.C. Yong, B. Jawan, Y.F. Cheng, H.L. Eng, Long-term results of living donor liver transplantation for glycogen storage disorders in children Liver transplantation : official publication of the American Association for the Study of Liver Diseases and the International Liver Transplantation Society 13 (2007) 848-852.

[14] A. Demaster, X.Y. Luo, S. Curtis, K.D. Williams, D.J. Landau, E.J. Drake, D.M. Kozink, A. Bird, B. Crane, F. Sun, C.R. Pinto, T.T. Brown, A.R. Kemper, D.D. Koeberl, Long-Term Efficacy Following Readministration of an Adeno-Associated Virus Vector in Dogs with Glycogen Storage Disease Type Ia Hum Gene Ther 23 (2012) 407-418.

[15] B. Crane, X. Luo, A. Demaster, K.D. Williams, D.M. Kozink, P. Zhang, T.T. Brown, C.R. Pinto, K. Oka, F. Sun, M.W. Jackson, L. Chan, D.D. Koeberl, Rescue administration of a helper-

dependent adenovirus vector with long-term efficacy in dogs with glycogen storage disease type Ia Gene Ther 19 (2012) 443-452.

[16] D.D. Koeberl, C. Pinto, B. Sun, S. Li, D.M. Kozink, D.K. Benjamin, Jr., A.K. Demaster, M.A. Kruse, V. Vaughn, S. Hillman, A. Bird, M. Jackson, T. Brown, P.S. Kishnani, Y.T. Chen, AAV vector-mediated reversal of hypoglycemia in canine and murine glycogen storage disease type Ia Molecular therapy : the journal of the American Society of Gene Therapy 16 (2008) 665-672.

[17] D.A. Weinstein, C.E. Correia, T. Conlon, A. Specht, J. Verstegen, K. Onclin-Verstegen, M. Campbell-Thompson, G. Dhaliwal, L. Mirian, H. Cossette, D.J. Falk, S. Germain, N. Clement, S. Porvasnik, L. Fiske, M. Struck, H.E. Ramirez, J. Jordan, K. Andrutis, J.Y. Chou, B.J. Byrne, C.S. Mah, Adeno-associated virus-mediated correction of a canine model of glycogen storage disease type Ia Hum Gene Ther 21 (2010) 903-910.

[18] X. Luo, G. Hall, S. Li, A. Bird, P.J. Lavin, M.P. Winn, A.R. Kemper, T.T. Brown, D.D. Koeberl, Hepatorenal correction in murine glycogen storage disease type I with a double-stranded adeno-associated virus vector Molecular therapy : the journal of the American Society of Gene Therapy 19 (2011) 1961-1970.

[19] K.J. Lei, H. Chen, C.J. Pan, J.M. Ward, B. Mosinger, Jr., E.J. Lee, H. Westphal, B.C. Mansfield, J.Y. Chou, Glucose-6-phosphatase dependent substrate transport in the glycogen storage disease type-1a mouse Nat Genet 13 (1996) 203-209.

[20] P.S. Kishnani, Y. Bao, J.Y. Wu, A.E. Brix, J.L. Lin, Y.T. Chen, Isolation and nucleotide sequence of canine glucose-6-phosphatase mRNA: identification of mutation in puppies with glycogen storage disease type Ia Biochemical and molecular medicine 61 (1997) 168-177.

[21] D. Fleenor, R. Arumugam, M. Freemark, Growth hormone and prolactin receptors in adipogenesis: STAT-5 activation, suppressors of cytokine signaling, and regulation of insulin-like growth factor I Hormone research 66 (2006) 101-110.

[22] R. Arumugam, D. Fleenor, M. Freemark, Lactogenic and somatogenic hormones regulate the expression of neuropeptide Y and cocaine- and amphetamine-regulated transcript in rat insulinoma (INS-1) cells: interactions with glucose and glucocorticoids Endocrinology 148 (2007) 258-267.

[23] K. Dheda, J.F. Huggett, S.A. Bustin, M.A. Johnson, G. Rook, A. Zumla, Validation of housekeeping genes for normalizing RNA expression in real-time PCR BioTechniques 37 (2004) 112-114, 116, 118-119.

[24] R. Arumugam, D. Fleenor, D. Lu, M. Freemark, Differential and complementary effects of glucose and prolactin on islet DNA synthesis and gene expression Endocrinology 152 (2011) 856-868.

[25] B. Sun, H. Zhang, L.M. Franco, S.P. Young, A. Schneider, A. Bird, A. Amalfitano, Y.T. Chen, D.D. Koeberl, Efficacy of an adeno-associated virus 8-pseudotyped vector in glycogen storage disease type II Molecular therapy : the journal of the American Society of Gene Therapy 11 (2005) 57-65.

[26] D. Laflamme, Development and validation of a body condition score system for dogs Canine Pract 22 (1997) 10-15.

[27] Y. Yamazaki, M. Yuguchi, S. Kubota, K. Isokawa, Whole-mount bone and cartilage staining of chick embryos with minimal decalcification Biotechnic & histochemistry : official publication of the Biological Stain Commission 86 (2011) 351-358.

[28] T.I. Cesena, T.X. Cui, G. Piwien-Pilipuk, J. Kaplani, A.A. Calinescu, J.S. Huo, J.A. Iniguez-Lluhi, R. Kwok, J. Schwartz, Multiple mechanisms of growth hormone-regulated gene transcription Mol Genet Metab 90 (2007) 126-133.

[29] Y. Chen, -T., Glycogen Storage Diseases., in: C.T. Scriver, A.L. Beaudet, W.S. Sly, D. Valle (Eds.), The Metabolic and Molecular Bases of Inherited Disease, McGraw-Hill, New York, 2001.

[30] A. Katsurada, N. Iritani, H. Fukuda, Y. Matsumura, N. Nishimoto, T. Noguchi, T. Tanaka, Effects of nutrients and hormones on transcriptional and post-transcriptional regulation of fatty acid synthase in rat liver European journal of biochemistry / FEBS 190 (1990) 427-433.

[31] K.A. Greer, L.M. Hughes, M.M. Masternak, Connecting serum IGF-1, body size, and age in the domestic dog Age 33 (2011) 475-483.

[32] L. Jaillardon, L. Martin, P. Nguyen, B. Siliart, Serum insulin-like growth factor type 1 concentrations in healthy dogs and dogs with spontaneous primary hypothyroidism Veterinary journal 190 (2011) e95-99.

[33] C. Le Stunff, A.M. Gronowski, P. Rotwein, Contrasting acute in vivo nuclear actions of growth hormone and prolactin Molecular and cellular endocrinology 121 (1996) 109-117.

[34] O. Torring, B. Isberg, H.E. Sjoberg, E. Bucht, A.L. Hulting, Plasma calcitonin, IGF-I levels and vertebral bone mineral density in hyperprolactinemic women during bromocriptine treatment Acta endocrinologica 128 (1993) 423-427.

[35] D. Fleenor, J. Oden, P.A. Kelly, S. Mohan, S. Alliouachene, M. Pende, S. Wentz, J. Kerr, M. Freemark, Roles of the lactogens and somatogens in perinatal and postnatal metabolism and growth: studies of a novel mouse model combining lactogen resistance and growth hormone deficiency Endocrinology 146 (2005) 103-112.

[36] B.A. Scheven, N.J. Hamilton, Longitudinal bone growth in vitro: effects of insulin-like growth factor I and growth hormone Acta endocrinologica 124 (1991) 602-607.

[37] J.D. Hanna, F. Santos, J.W. Foreman, J.C. Chan, V.K. Han, Insulin-like growth factor-I gene expression in the tibial epiphyseal growth plate of growth hormone-treated uremic rats Kidney international 47 (1995) 1374-1382.

[38] R.C. Olney, J. Wang, J.E. Sylvester, E.B. Mougey, Growth factor regulation of human growth plate chondrocyte proliferation in vitro Biochemical and biophysical research communications 317 (2004) 1171-1182.

[39] J. Wang, J. Zhou, C.A. Bondy, Igf1 promotes longitudinal bone growth by insulin-like actions augmenting chondrocyte hypertrophy Faseb J 13 (1999) 1985-1990.

[40] F. Long, K.S. Joeng, S. Xuan, A. Efstratiadis, A.P. McMahon, Independent regulation of skeletal growth by Ihh and IGF signaling Developmental biology 298 (2006) 327-333.

[41] C. Trivin, J.C. Souberbielle, G. Aubertin, E. Lawson-Body, L. Adan, R. Brauner, Diagnosis of idiopathic growth hormone deficiency: contributions of data on the acid-labile subunit, insulin-like growth factor (IGF)-I and-II, and IGF binding protein-3 Journal of pediatric endocrinology & metabolism : JPEM 19 (2006) 481-489.

[42] S. Cianfarani, A. Liguori, S. Boemi, M. Maghnie, L. Iughetti, M. Wasniewska, M.E. Street, S. Zucchini, G. Aimaretti, D. Germani, Inaccuracy of insulin-like growth factor (IGF) binding protein (IGFBP)-3 assessment in the diagnosis of growth hormone (GH) deficiency from childhood to young adulthood: association to low GH dependency of IGF-II and presence of circulating IGFBP-3 18-kilodalton fragment The Journal of clinical endocrinology and metabolism 90 (2005) 6028-6034.

[43] E. Ferrante, C. Giavoli, S. Porretti, E. Vassallo, C.L. Ronchi, A.G. Lania, P. Beck-Peccoz, A. Spada, Evaluation of the components of the insulin-like growth factors system in GH-deficient adults: effects of twelve-month rhGH treatment Hormone and metabolic research = Hormon- und Stoffwechselforschung = Hormones et metabolisme 38 (2006) 352-355.

[44] D.B. Dunger, A.T. Holder, J.V. Leonard, J. Okae, M.A. Preece, Growth and endocrine changes in the hepatic glycogenoses European journal of pediatrics 138 (1982) 226-230.

[45] T. Zoetis, M.S. Tassinari, C. Bagi, K. Walthall, M.E. Hurtt, Species comparison of postnatal bone growth and development Birth defects research. Part B, Developmental and reproductive toxicology 68 (2003) 86-110.

[46] B. Clancy, R.B. Darlington, B.L. Finlay, Translating developmental time across mammalian species Neuroscience 105 (2001) 7-17.

[47] L.E. Case, D.D. Koeberl, S.P. Young, D. Bali, S.M. DeArmey, J. Mackey, P.S. Kishnani, Improvement with ongoing Enzyme Replacement Therapy in advanced late-onset Pompe disease: a case study Mol Genet Metab 95 (2008) 233-235.

[48] W.H. Yiu, Y.M. Lee, W.T. Peng, C.J. Pan, P.A. Mead, B.C. Mansfield, J.Y. Chou, Complete normalization of hepatic G6PC deficiency in murine glycogen storage disease type Ia using gene therapy Molecular therapy : the journal of the American Society of Gene Therapy 18 (2010) 1076-1084.

FIGURE LEGENDS

Fig. 1. Decreased GH, IGF 1, and hepatic receptors for GH, prolactin and IGF 1 in *G6pase* (-/-) mice. (A) Randomly sampled plasma growth hormone in *G6pase* (-/-) mice, either untreated (UT; n=3) or glucose treated (GT; n=4) and for *G6pase* (+/+) littermates (WT; n=3). (B) Plasma IGF 1 for WT mice and for GT *G6pase* (-/-) mice at 2 weeks of age (n=3 in each group). (C) Realtime RT-PCR analysis of liver RNA from 13 +/- 1-day-old *G6pase* (-/-) and unaffected *G6pase* (+/+ and +/-) littermates for the GH receptor (GHR-L) and prolactin receptor (PRLR-L) (n=4 in each group), and for IGF 1 and IGF 2 RNA (n=3 for each group) in the liver of GT *G6pase* (-/-) and WT mice, units are normalized to β-actin. Mean +/- standard deviation shown. ** = $p<0.01$, *** = $p<0.001$ (as determined by two-tailed homoscedastic Student's *t*-test).

Figure 2. GH signaling pathway in *G6pase (-/-)* liver. (A) Western blot detection of fatty acid synthetase (FASN), c-Fos, and STAT5 in glucose-treated (GT) *G6pase* (-/-) mouse and *G6pase* (+/+) mouse (WT) liver at 13 +/- 1 days of age. Each lane represents an individual mouse. (B) Quantification of the indicated proteins by densitometry of Western blot images, normalized to β-actin. The normalized signals for GT, UT, and WT mouse liver are shown (mean +/- SD). (C) Body weight at 10 days of age for GH treated and untreated mice. Groups were unaffected, (*G6pase* (+/-) and *G6pase* (+/+), (n=4) and affected, *G6pase* (-/-), (n=5) mice. (D) Realtime RT-PCR analysis of liver RNA from 13 +/- 1-day-old *G6pase* (-/-) (n=8) and both *G6pase* (+/-) and *G6pase* (+/+) mice (n=8) following glucose and GH treatment (GT) for growth hormone receptor (GHR-L), prolactin receptor (PRLR-L), IGF 1, IGF 2, and insulin receptor (Ins Rec) RNA (n=4 for each group), normalized to β-actin. Half of the mice in each group were injected with 10 μg GH for 7 days, and half of the mice were treated similarly with 25 μg daily. The responses for the two dosages were equivalent, and therefore results were pooled for the two GH treatments. * = $p<0.05$; ** = $p<0.01$, *** = $p<0.001$ (as determined by two-tailed homoscedastic Student's *t*-test) for the comparisons of *G6pase* (-/-) mice with normal, WT or with unaffected mice. The latter

group of unaffected mice included both *G6pase* (+/-) and *G6pase* (+/+) mice (see Methods for further information).

Figure 3. Growth and IGF 1 in *G6pase (-/-)* mice following AAV2/9-G6Pase vector administration. Affected mice did not survive until 1 month of age unless the AAV vector was administered. (A) Weight of *G6pase* (+/+) mice (n=4) and *G6pase* (-/-) mice (n=7) following administration of the AAV2/8-G6Pase vector ($1x10^{13}$ vector particles/kg body weight) at 2 weeks of age. (B) Plasma IGF 1 for *G6pase* (+/+) and *G6pase* (-/-) mice (n=4 in each group), either untreated or following AAV2/8-G6Pase vector administration, respectively. * = $p<0.05$ (as determined by two-tailed homoscedastic Student's *t*-test).

Fig. 4. Decreased growth and IGF 1 in GSD-Ia affected dogs following AAV vector administration and GSD-Ia carriers compared with wild-type littermates. Body weights obtained during the first 7 weeks of life and at >20 months of age. (A) GSD-Ia affected animals were either treated with AAV2/9-G6Pase at 2-3 days of life or received no treatment and were managed with frequent meals and glucose administration alone. (B) Unaffected animals were littermates of GSD-Ia affected offspring and were either wild-type or heterozygous carriers of GSD-Ia. No significant difference in early weight gain in GSD-Ia carriers and wild-type dogs ($p>0.11$ for all time points), therefore they were grouped together here. GSD-Ia affected animals were treated with AAV2/9-G6Pase at 2-3 days of life. (C) Weight (kg) obtained at 20 months of age and older from GSD-Ia affected dogs treated with AAV2/9-G6Pase as neonates and their unaffected littermates, including wild-type and carriers for GSD-Ia. Mean +/- standard deviation shown. * = $p<0.05$; ** = $p<0.01$, *** = $p<0.001$ (as determined by one-tailed heteroscedastic Student's *t*-test and one way ANOVA with Tukey analysis); n=2-22, see Table S1. (D) Serum IGF 1 concentrations at 8 weeks and 22-23 weeks of age in GSD-Ia affected dogs treated with AAV2/9-G6Pase as neonates and their unaffected littermates, including wild-type and carriers for GSD-Ia. Mean ± standard deviation shown. * = $p<0.05$; *** = $p<0.001$ as determined by one

way between subjects ANOVA at 8 weeks and Student's t-test between carriers and GSD-Ia AAV2/9-G6Pase treated; one wild-type dog was adopted prior to 20 weeks accounting for n=1 at 22-23 weeks.

Fig. 5. Dyschondrogenesis of *G6pase* (-/-) mice at 12 days of age. Alcian Blue/Alizarin Red whole limb staining of 12-day old glucose treated *G6pase* (-/-) mice (n=3) and *G6pase* (+/+) mice (n=3). Images representative of all animals analyzed. (A) Hip shows delay in secondary ossification in *G6pase* (-/-) mice. (B) Knee of *G6pase* (-/-) mice demonstrates severe delay in secondary ossification and malformation of distal femur and proximal tibia. (C) Elbow of *G6pase* (-/-) mouse demonstrates delay in ossification and deformity of proximal radius and ulna. Cartilage stains blue and bone stains red/pink. Scale bar = 1mm. Craniad to the left of the images and proximal at the top.

Fig. 6. Delayed ossification of *G6pase* (-/-) mice and dysplasia in AAV2/8-G6Pase vector-treated *G6pase* (-/-) mice. Radiographic images taken of untreated *G6pase* (-/-) mice (n=3) and *G6pase* (+/+) mice (n=3) at 12 days of age and AAV2/8-G6Pase vector-treated *G6pase* (-/-) mice with *G6pase* (+/+) mice at 6 months of age. Images representative of all animals analyzed. (A) Hip, (B) knee, (C) caudal vertebrae 4-6, (D) shoulder, (E) elbow, and (F) carpus demonstrate severe dysplasia and delayed secondary ossification in *G6pase* (-/-) mice.

Fig. 7. Decreased bone dimensions in GSD-Ia affected dogs treated with AAV2/9-G6Pase compared with unaffected littermates. (A) Mediolateral radiographic view taken of forelimb at 3 months of age from a GSD-Ia male affected dog (right) treated with AAV2/9-G6Pase, his wild-type male littermate (left), and a female GSD-Ia carrier from a different litter (middle). Note a 65% difference in radius length of the GSD-Ia affected dog treated with AAV2/9-G6Pase and wild-type littermate, versus a 78% difference between GSD-Ia carrier and wild-type (see Table S3). Dogs weighed 3.9 kg (A), 3.2 kg (B) and 1.8 kg (C) at time radiographs were taken. White

marker represents 15 mm. (B) Photograph of 34-month-old female GSD-Ia AAV2/9-G6Pase vector-treated dog (right) and male GSD-Ia carrier littermate (left) who weighed 8.2 kg at the time the picture was taken. (C-E) Radiographic analysis performed at 37 months of age of same female GSD-Ia AAV2/9-G6Pase treated dog (right) and a different male GSD-Ia carrier littermate (left). Dogs weighed 3.8 kg and 8.6 kg, respectively, at time of radiographs. White marker represents 15 mm. (C) Plantardorsal radiographic view of the right rear foot, metatarsals and proximal phalangeal bones of a female GSD-Ia AAV-G6Pase treated dog were approximately 88 and 87%, respectively, the length of her male GSD-Ia carrier littermate. (D) Lateral radiographic view of the femur of a female GSD-Ia AAV-G6Pase treated dog were approximately 88% the length of those of her male GSD-Ia carrier littermate, but 70% the width. (E) Ventrodorsal radiographic view of the pelvis of a female GSD-Ia AAV-G6Pase treated dog were approximately 82% and 76% the length and width, respectively, of the pelvis of her male GSD-Ia carrier littermate (see Table S4).

Supplemental Figure 1. Decreased bone length of *G6pase* (-/-) mice at 12 days and in AAV2/8-G6Pase vector-treated *G6pase* (-/-) mice at 6 months. Bone measurements from calibrated radiographic images of 12 day old (12d) untreated *G6pase* (-/-) mice and 6 month old (6m) *G6pase* (-/-) mice that were treated with AAV2/8-G6Pase at 2 weeks of age. *G6pase* (+/+) mice at the same ages are present for comparison; n=3 mice/group. Mean +/- standard deviation shown. * = $p<0.05$ (as determined by Kruskal-Wallis Test) (A) Length (mm) of extremity long bones. All individual bone length data for 12d old mice were significantly less than for respective 6m old mice data (Kruskal-Wallis Test, $p<0.01$). (B) Length (mm) of metatarsals (MT), and proximal (P1) and middle (P2) phalanges of the third (III) and fifth (V) toe. All individual bone length data for 12d old mice were significantly less than for respective 6m old mice data (Kruskal-Wallis Test, $p<0.01$). (C) Length and width of craniad and caudad components of the axial skeleton, cranially the length and width of the head and length of the third cervical vertebra (C3), and caudally, the length of the sixth lumbar vertebra (L6), and the

length of the ilium and ischium and width of the pelvis from iliac crest-iliac crest (IC-IC). # = $p<0.05$ 6-month-old mice measurements significantly greater than 12-day old mice as determined by the Kruskal-Wallis test.

Table 1. Analysis of gene expression in mouse liver by quantitative real time PCR. The table shows the oligonucleotide primer pairs, all of which encode mouse genes. The mean CT values shown in the table were obtained from liver samples of wild-type mice.

mGene	Accession #	Primers (top forward, bottom reverse)	Mean CT values
PRLR-L	**NM_001034111**	5' CCT GCA TCT TTC CAC CAG TTC 3' 5' GCA CTC AGC AGT TCT TCA GAC TTG 3'	**24**
GHR-L	**NM_017094**	5' CCA GTT TCC ATG GTT CTT AAT TAT TAT 3' 5' ATC TTA ATC CTT TGC TGC TTT GAA AA 3'	**22**
Insulin receptor	**NM_010568**	5' GCA GTG TGG CAG CCT ACG T3' 5' CAG GGC CAA CGA TGT CAT CT 3'	**23**
IGF 1	**NM_010512**	5' CCA CAC TGA CAT GCC CAA GAC 3' 5' TGC AGC TTC GTT TTC TTG TTT G 3'	**21**
IGF 2	**NM_010514**	5' TGT CTA CCT CTC AGG CCG TAC TT 3' 5' CCA GGT GTC ATA TTG GAA GAA CTT G 3'	**17**
Acidic Riboprotein - PO	**NM_007475**	5' CCC TGA AGT GCT CGA CAT CA 3' 5' GCG GAC ACC CTC CAG AAA GC 3'	**21**

Figure 1

Click here to download high resolution image

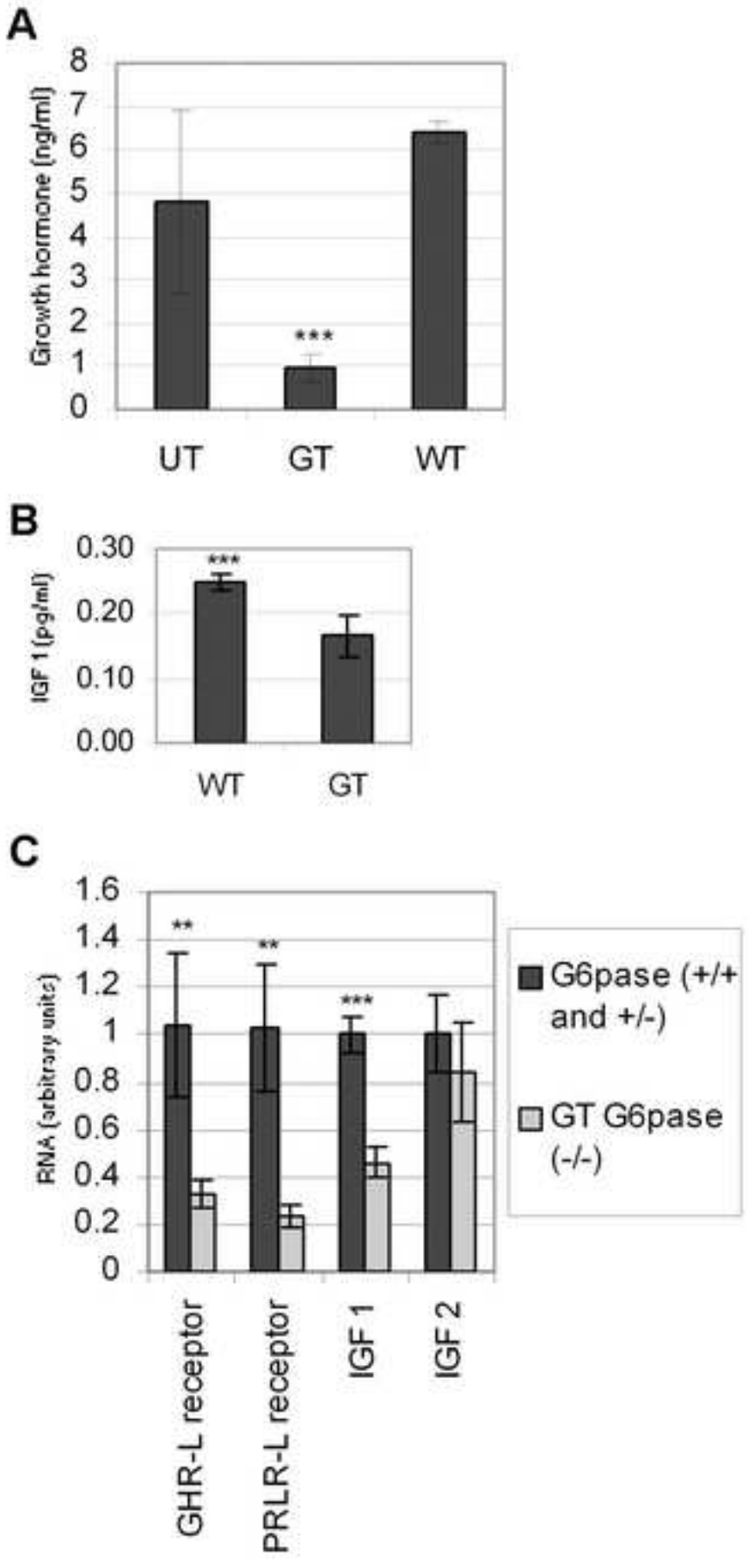

Figure 2

Click here to download high resolution image

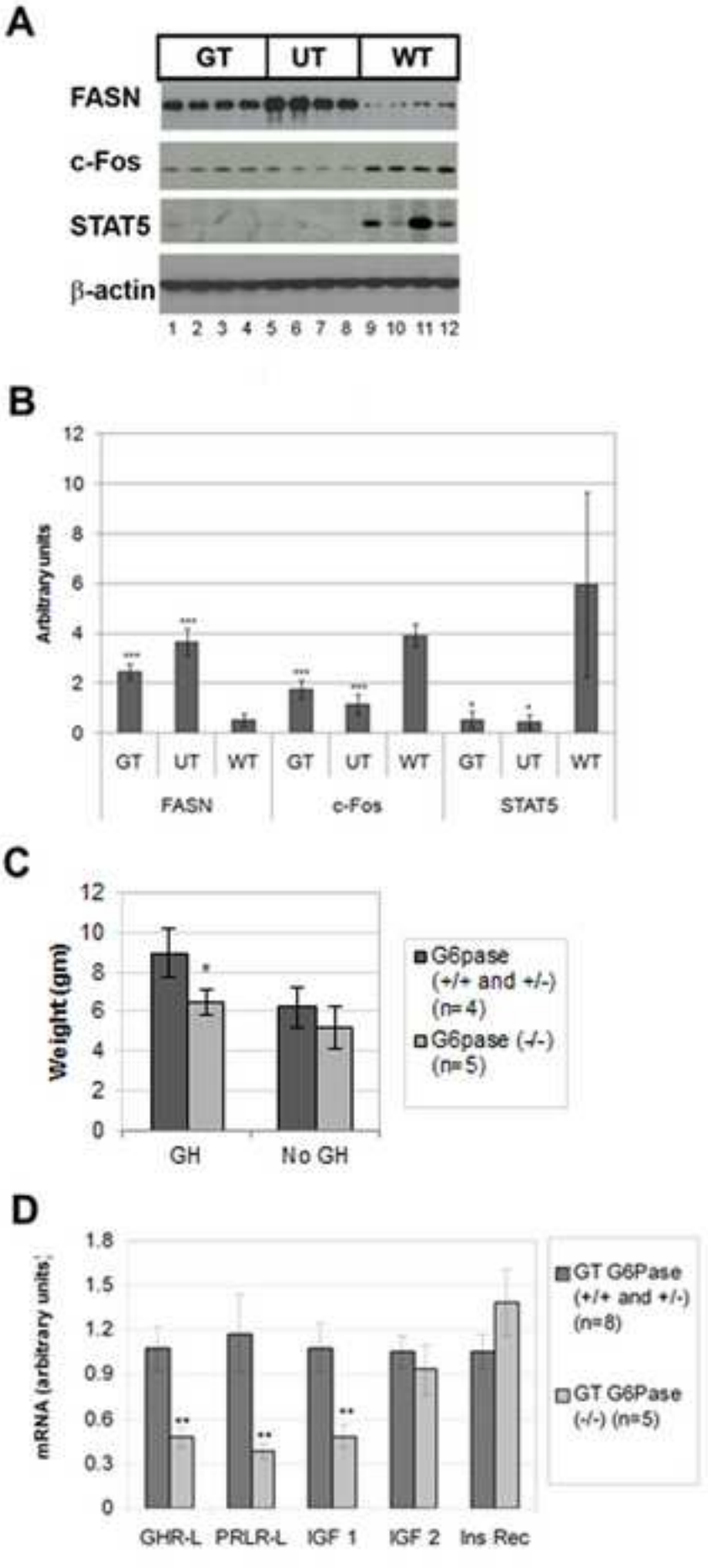

Figure 3

Click here to download high resolution image

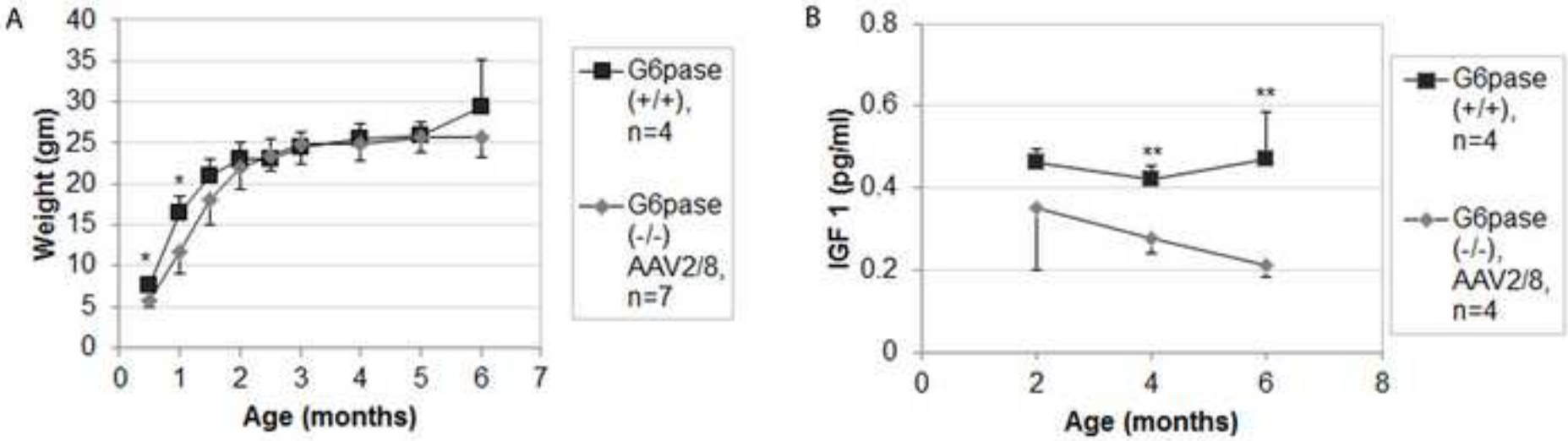

Figure 4

Click here to download high resolution image

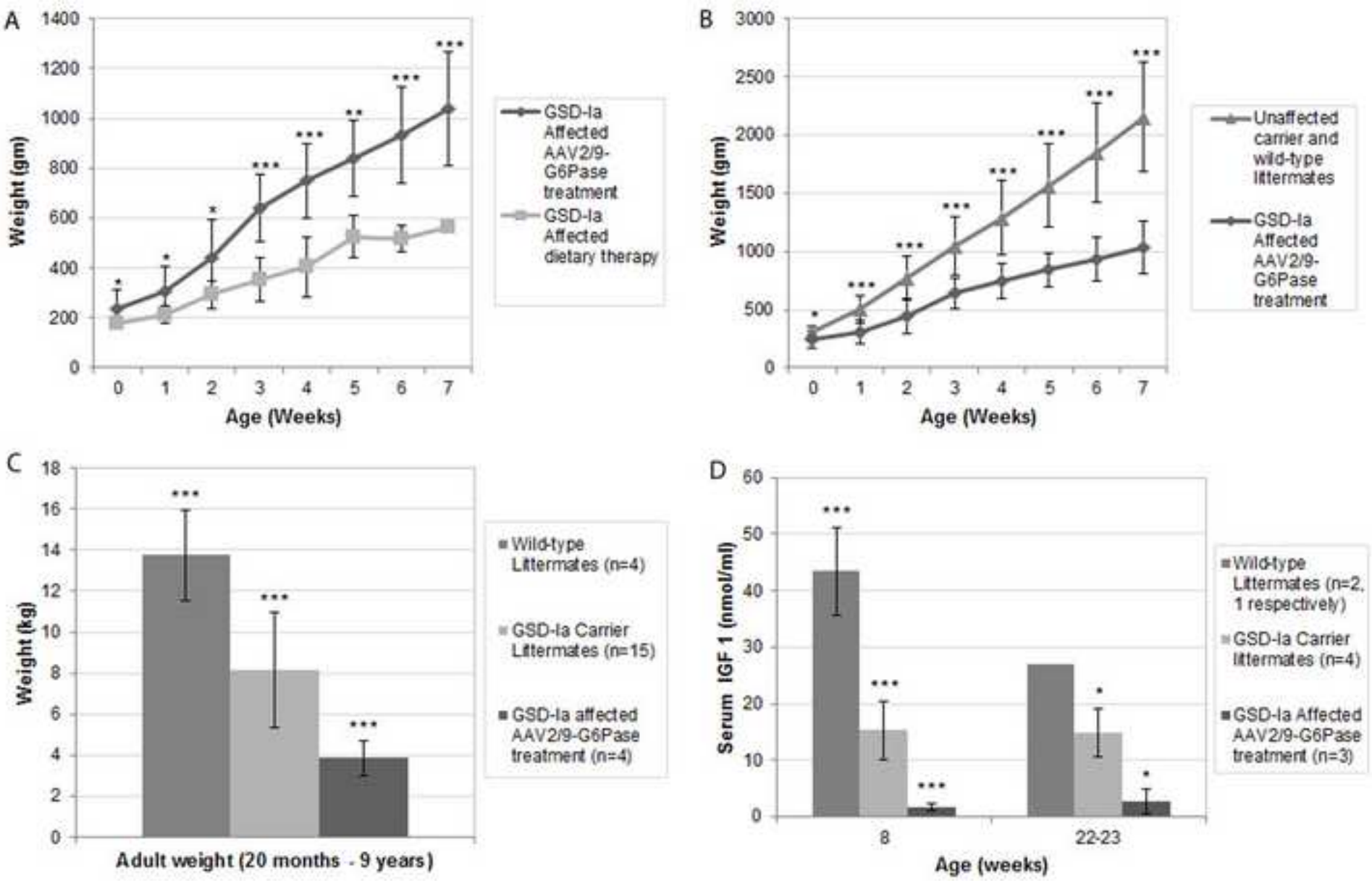

Figure 5

Click here to download high resolution image

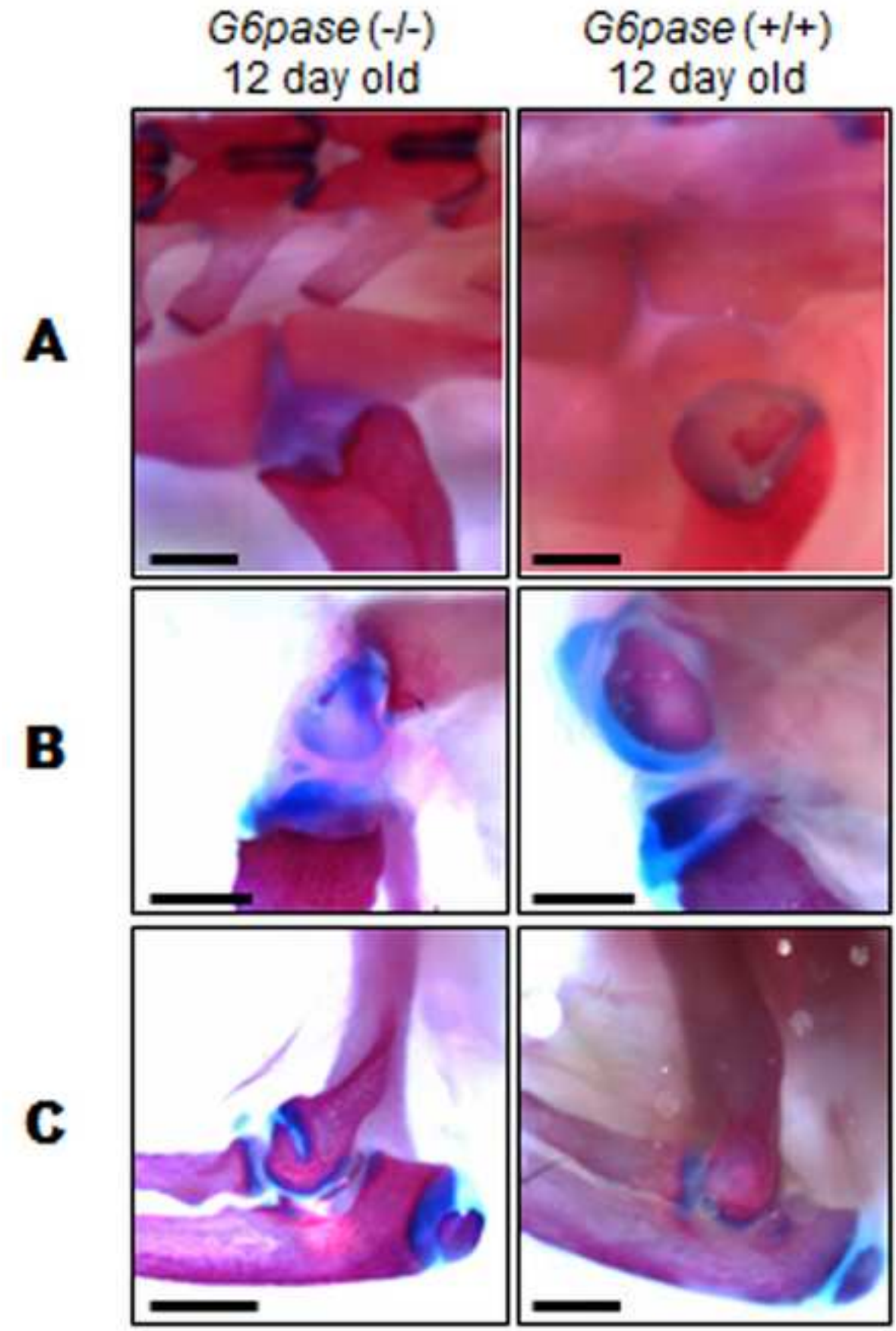

Figure 6

Click here to download high resolution image

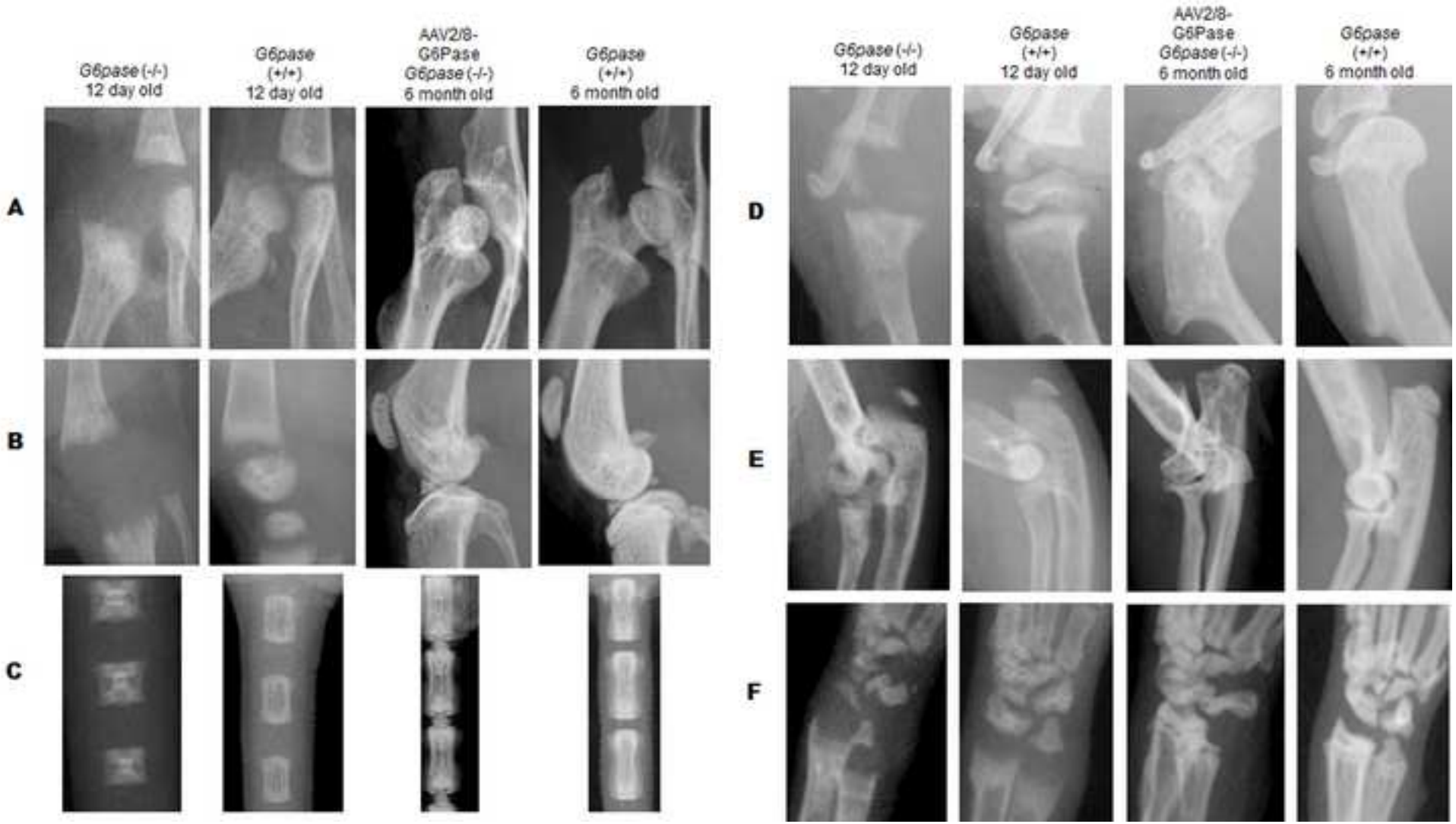

Figure 7

Click here to download high resolution image

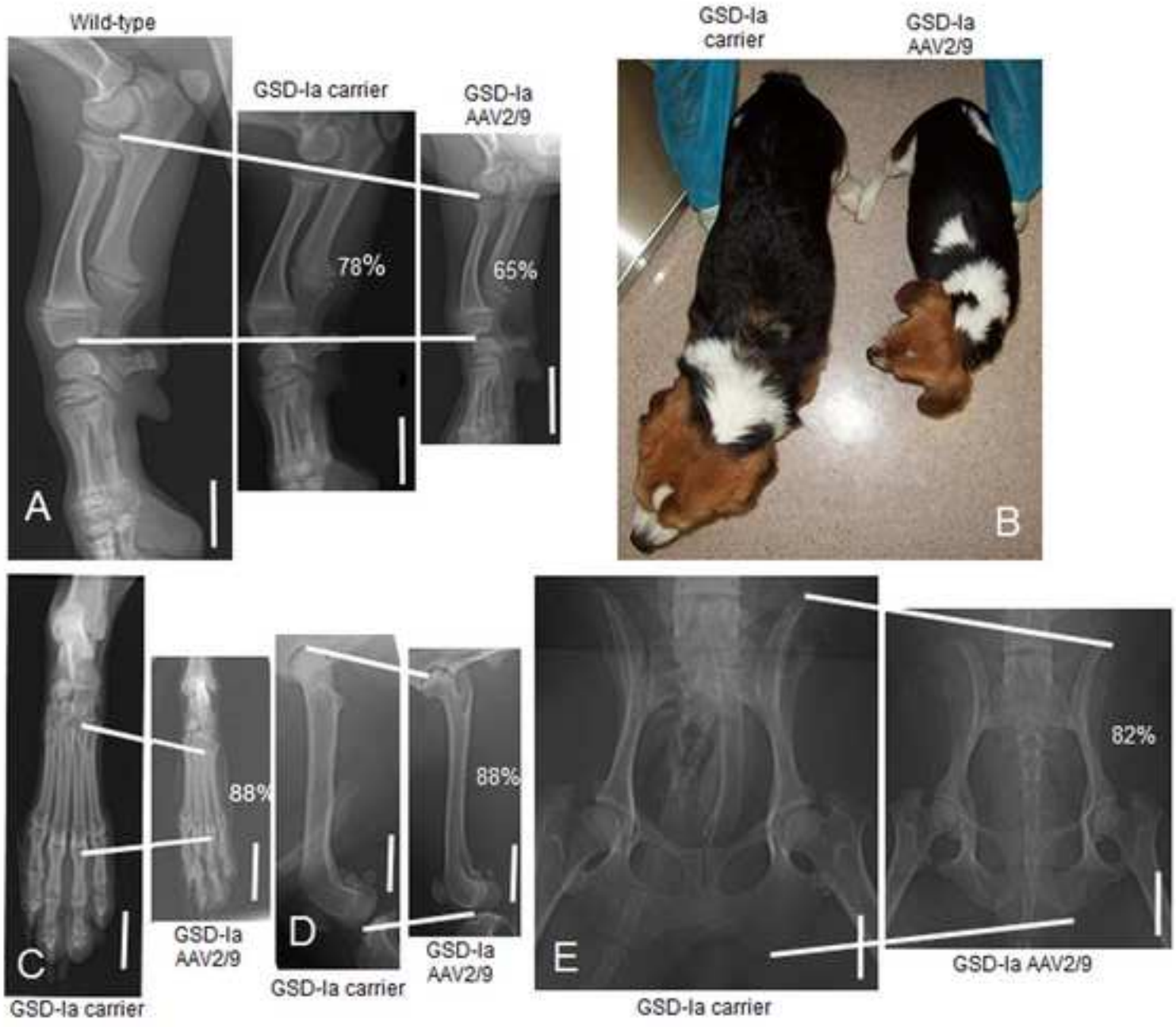

Supplemental table 1

Click here to download Supplementary Material: Supplemental Table 1.docx

Supplementary Table 2

Click here to download Supplementary Material: Supplemental Table 2.docx

Supplemental Table 3

Click here to download Supplementary Material: Supplemental Table 3.docx

Supplemental Table 4

Click here to download Supplementary Material: Supplemental Table 4.docx

Supplemental figure 1

Click here to download Supplementary Material: Sup Fig 1.jpg